International Journal of Modern Physics B
Vol. 27, No. 14 (2013) 1350065 (15 pages)

DOI: 10.1142/S0217979213500653

World Scientific
www.worldscientific.com

CROSSOVER FROM SPONTANEOUSLY GENERATED COHERENCE TO AUTLER–TOWNES SPLITTING IN THREE-LEVEL ATOMIC SYSTEMS

QIONG DU, CHAO HANG and GUOXIANG HUANG*

State Key Laboratory of Precision Spectroscopy and Department of Physics, East China Normal University, Shanghai 200062, P. R. China

**gxhuang@phy.ecnu.edu.cn*

Received 26 January 2013
Accepted 26 February 2013
Published 9 May 2013

We investigate spontaneously generated coherence (SGC) and Autler–Townes Splitting (ATS) in various three-level systems. Through detailed analytical calculations on absorption spectrum of probe laser field, we show that in V-type system the SGC can completely eliminate the absorption of the probe field and at the same time significantly reduce the group velocity. By using residue theorem and spectrum decomposition method, we prove that there exists a crossover from SGC to ATS for both cold and warm atoms when the magnitude of SGC is changed. Different contributions of SGC and ATS to probe-field absorption spectrum are clearly clarified in different parameter regions. In addition, our results show that there is no SGC and hence no SGC-ATS crossover in Λ- and Ξ-type systems.

Keywords: Spontaneously generated coherence; Autler–Townes splitting; SGC-ATS crossover.

PACS numbers: 32.80.Qk, 42.50.Gy, 42.65.An

1. Introduction

Quantum interference effect is an important subject of many studies due to their important applications in quantum computing and information processing. In multilevel atomic systems, due to the quantum interference effect induced by a control laser field, the absorption of a probe laser field can be largely eliminated even if it is tuned to a very strong one-photon transition. Such phenomenon, called electromagnetically induced transparency (EIT),[1] can result in a significant reduction of group velocity and a giant enhancement of Kerr nonlinearity. Based on these striking features, EIT has been used to realize slow light, quantum memory,[2] quantum phase gates,[3,4] ultraslow optical solitons,[5,6] and so on.

However, in EIT media it is crucial to have at least two laser fields, i.e., a control field and a probe field. In addition, optical absorption of the probe field cannot

be eliminated especially for warm atoms, which can result in significant attenuation of the probe field for long propagation distance. It is noteworthy that, besides EIT, another important type of quantum interference phenomenon, known as spontaneously generated coherence (SGC), exists.[7] The quantum interference in SGC media occurs between two spontaneous emission channels without using any control field. In recent years, much attention has been paid to the study of SGC and related topics, including lasing without inversion,[8–11] coherent population trapping,[12] spectral narrowing and fluorescence quenching,[13–17] adiabations,[18] fluorescence squeezing,[19] giant self-phase modulation,[20] ground-state quantum beats,[21] cavity-mode entanglement,[22] electromagnetically induced grating[23] ultraslow optical solitons[24] etc.

In SGC media, a significant dip in probe-field absorption spectrum may appear, which is similar to the phenomenon known as the Autler–Townes splitting (ATS),[25,26] which is not a quantum interference phenomenon. Thus, it is important to clarify the relation and distinction between SGC and ATS. In this article, we investigate the SGC and ATS in resonant three-level atomic systems, and give a definite answer to when the detected reduction in absorption is a result of SGC, when of ATS, and when of the joint contribution from SGC and ATS. Through detailed analytical calculations on probe-field absorption spectrum, we show that in V-type system the SGC can completely eliminate the absorption and at the same time significantly reduce the group velocity. By using residue theorem and spectrum decomposition method, we find that there exists a crossover region from SGC to ATS (called SGC-ATS crossover for short) for both cold and warm atoms when we change the magnitude of SGC. Different contributions of SGC and ATS to the probe-field absorption spectrum are clearly clarified in different parameter regions. Additionally, our results show that there is no SGC and hence no SGC-ATS crossover in Λ- and Ξ-type systems.

The rest of the article is arranged as follows. In Sec. 2, the model of three-level V-type configuration with SGC is introduced. Linear dispersion and absorption properties are analyzed based on full density matrix calculations. The existence of crossover from SGC to ATS in this system is demonstrated. Different contributions of SGC and ATS are clarified in different regions for both cold and warm atoms. In Sec. 3, the same analysis is carried out for models of three-level Λ- and Ξ-type configurations. We find no SGC and hence no SGC-ATS crossover in Λ- and Ξ-type systems. Finally, the last section contains a summary of our main results.

2. SGC-ATS Crossover in V-Type System

2.1. *Model*

We consider a three-level V-type atomic system, shown in Fig. 1(a), in which two closely spaced excited states $|2\rangle$ and $|3\rangle$ decay simultaneously into the ground state $|1\rangle$ by the spontaneous emission with decay rates Γ_2 and Γ_3, respectively. The quantum interference between two decay channels (i.e., $|2\rangle$ to $|1\rangle$ and $|3\rangle$ to $|1\rangle$) results

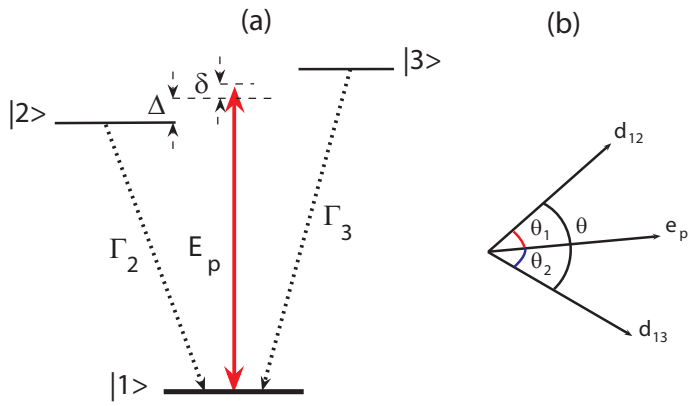

Fig. 1. (a) Energy level diagram and excitation scheme of a three-level V-type system with SGC. $|j\rangle$ $(j = 1, 2, 3)$ are atomic bare states, $\mathbf{E}_p$ is probe field, Δ and δ are detunings, and Γ_j $(j = 1, 2)$ are decay rates of relevant states. (b) The alignment of dipole matrix elements $\mathbf{d}_{12}$ and $\mathbf{d}_{13}$ and the unit polarization vector of the probe field $\mathbf{e}_p$. θ_1 (θ_2) is the angle between $\mathbf{d}_{12}$ $(\mathbf{d}_{13})$ and $\mathbf{e}_p$. $\theta = \theta_1 + \theta_2$ is the angle between $\mathbf{d}_{12}$ and $\mathbf{d}_{13}$.

in the SGC of the system.[27] A weak probe field of frequency ω_p and wavevector $\mathbf{k}_p$, i.e., $\mathbf{E}_p(\mathbf{r}, t) = \mathbf{e}_p\mathcal{E}_p(\mathbf{r}, t)e^{i(\mathbf{k}_p\cdot\mathbf{r}-\omega_p t)} + \text{c.c}$, couples the ground state $|1\rangle$ to excited states $|2\rangle$ and $|3\rangle$, where $\mathbf{e}_p$ and $\mathcal{E}_p(\mathbf{r}, t)$ are the unit polarization vector and the envelope function of the probe field, respectively.

Under electric-dipole, rotating-wave, and Weisskopf–Wigner approximations, the equations of motion for the density matrix governing atomic dynamics are:

$$\dot{\rho}_{11} = \Gamma_2\rho_{22} + \Gamma_3\rho_{33} - i\Omega_p\rho_{12} + i\Omega_p^*\rho_{21} - ip\Omega_p\rho_{13} + ip\Omega_p^*\rho_{31} + \eta\sqrt{\Gamma_2\Gamma_3}(\rho_{23} + \rho_{32}), \tag{1}$$

$$\dot{\rho}_{22} = -\Gamma_2\rho_{22} + i\Omega_p\rho_{12} - i\Omega_p^*\rho_{21} - \eta\frac{\sqrt{\Gamma_2\Gamma_3}}{2}(\rho_{23} + \rho_{32}), \tag{2}$$

$$\dot{\rho}_{33} = -\Gamma_3\rho_{33} + ip\Omega_p\rho_{13} - ip\Omega_p^*\rho_{31} - \eta\frac{\sqrt{\Gamma_2\Gamma_3}}{2}(\rho_{23} + \rho_{32}), \tag{3}$$

$$\dot{\rho}_{21} = \left[i(\Delta + \delta) - \frac{\Gamma_2}{2}\right]\rho_{21} + i\Omega_p(\rho_{11} - \rho_{22}) - ip\Omega_p\rho_{23} - \eta\frac{\sqrt{\Gamma_2\Gamma_3}}{2}\rho_{31}, \tag{4}$$

$$\dot{\rho}_{31} = \left[i(-\Delta + \delta) - \frac{\Gamma_3}{2}\right]\rho_{31} + ip\Omega_p(\rho_{11} - \rho_{33}) - i\Omega_p\rho_{32} - \eta\frac{\sqrt{\Gamma_2\Gamma_3}}{2}\rho_{21}, \tag{5}$$

$$\dot{\rho}_{32} = -\left(i2\Delta + \frac{\Gamma_2 + \Gamma_3}{2}\right)\rho_{32} - i\Omega_p^*\rho_{31} + ip\Omega_p\rho_{12} - \eta\frac{\sqrt{\Gamma_2\Gamma_3}}{2}(\rho_{22} + \rho_{33}), \tag{6}$$

where $\Omega_p = \mathbf{e}_p \cdot \mathbf{d}_{12}\mathcal{E}_p/\hbar$ is half Rabi frequency of the probe field with $\mathbf{d}_{ij} \equiv \langle i|\mathbf{d}|j\rangle$ being density-matrix elements related to states $|i\rangle$ and $|j\rangle$, $\Delta = (E_3 - E_2)/(2\hbar)$ is half frequency difference between $|2\rangle$ and $|3\rangle$, and $\delta = -\mathbf{k}_p \cdot \mathbf{v} + \omega_p - (E_3 + E_2)/(2\hbar)$

is one-photon detuning [see Fig. 1(a)] with $\mathbf{v}$ being the velocity of atoms. The cross coupling term contributed by the SGC effect is manifested by the factor $\eta\sqrt{\Gamma_2\Gamma_3}/2$, with $\eta = \mathbf{d}_{12}\cdot\mathbf{d}_{13}/|\mathbf{d}_{12}||\mathbf{d}_{13}| = \cos\theta$ denoting the alignment of two dipole matrix elements $\mathbf{d}_{12}$ and $\mathbf{d}_{13}$, where θ is the misalignment angle between $\mathbf{d}_{12}$ and $\mathbf{d}_{13}$ [see Fig. 1(b)]. If $\mathbf{d}_{12}$ and $\mathbf{d}_{13}$ are parallel (i.e. $\theta = 0$), one has $\eta = 1$, the system exhibits maximum SGC; if $\mathbf{d}_{12}$ and $\mathbf{d}_{13}$ are perpendicular (i.e. $\theta = \pi/2$), one has $\eta = 0$, the system displays no SGC. $p = |\mathbf{e}_p\cdot\mathbf{d}_{13}|/|\mathbf{e}_p\cdot\mathbf{d}_{12}| = |\mathbf{d}_{13}|\cos\theta_1/[|\mathbf{d}_{12}|\cos\theta_2]$, where θ_1 (θ_2) is the misalignment angle between $\mathbf{d}_{12}$ ($\mathbf{d}_{13}$) and $\mathbf{e}_p$.

The equation of motion for Ω_p can be obtained by using Maxwell equation. The electric polarization intensity of the system is given by:

$$\mathbf{P} = \mathcal{N}_a\int_{-\infty}^{\infty} dv f(v)\{\mathbf{p}_{12}\sigma_{21}\exp[i(k_p z-\omega_p t)] + p\mathbf{p}_{13}\sigma_{31}\exp[i(k_p z-\omega_p t)] + \text{c.c.}\} \tag{7}$$

where $\mathcal{N}_a$ is atomic density and $f(v)$ is the atomic velocity distribution. In deriving above equation, we have assumed $\mathbf{k}_p$ is along z-direction. In thermal equilibrium, the velocity distribution profile is Gaussian, i.e.,

$$f(v) = \frac{1}{\sqrt{\pi}v_T}e^{-(v/v_T)^2}, \tag{8}$$

where $v_T = \sqrt{2k_BT/M}$ is the most probable atomic speed at temperature T. Under slowly-varying envelope approximation, the Maxwell equation reads:

$$i\left(\frac{\partial}{\partial z}+\frac{1}{c}\frac{\partial}{\partial t}\right)\Omega_p + \int_{-\infty}^{\infty} dv f(v)(\kappa_{12}\rho_{21}+\kappa_{13}p\rho_{31}) = 0, \tag{9}$$

where $\kappa_{12} = \mathcal{N}_a\omega_p|\mathbf{e}_p\cdot\mathbf{d}_{12}|^2/(2\epsilon_0 c\hbar)$ and $\kappa_{13} = \mathcal{N}_a\omega_p|\mathbf{e}_p\cdot\mathbf{d}_{13}|^2/(2\epsilon_0 c\hbar)$.

Since $|2\rangle$ and $|3\rangle$ are closely spaced, for simplicity we assume that $|\mathbf{d}_{13}| \simeq |\mathbf{d}_{12}|$. In addition, a particular case can be found that θ is equally partitioned by $\mathbf{e}_p$, i.e., $\theta_1 = \theta_2 \equiv \theta/2$, as did in Ref. 23. Under above considerations, we take $\Gamma_2 \approx \Gamma_3 \equiv \Gamma$, $\kappa_{12} \simeq \kappa_{13} \equiv \kappa$ and $p = 1$.

2.2. *Cold atoms*

We first consider the V-type system for cold atoms. In this case one should take $v \to 0$ in Eqs. (1)–(6) and $f(v) \to \delta(v)$ in Eq. (9). When the probe field is absent, the steady-state solution of the system reads $\rho_{11}^{(0)} = 1$ and $\rho_{22}^{(0)} \simeq \rho_{33}^{(0)} \simeq \rho_{32}^{(0)} = 0$.

The linear optical response of the system can be obtained by solving the Maxwell–Bloch (MB) Eqs. (1)–(6) and (9). Assuming ρ_{21}, ρ_{31} and Ω_p are small quantities proportional to $\exp\{i[K_V(\omega)z-\omega t]\}$, we obtain the linear dispersion relation:

$$K_V(\omega) = \frac{\omega}{c} - \kappa\frac{2\omega + i(1-\eta)\Gamma}{D_V(\omega)}, \tag{10}$$

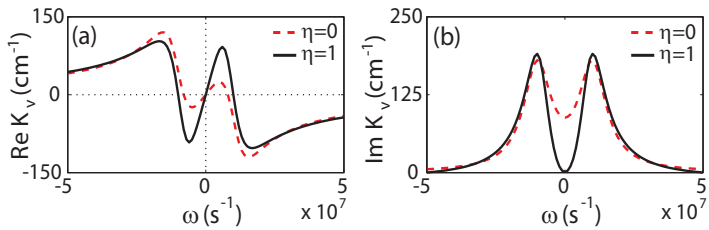

Fig. 2. (a) Re K_V and (b) ImK_V as functions of ω with the maximum SGC ($\eta = 1$; the solid line) and without SGC ($\eta = 0$; the dashed line).

where $D_V(\omega) = (\omega + \Delta + i\Gamma/2)(\omega - \Delta + i\Gamma/2) + \eta^2\Gamma^2/4$. For deriving (10), we have set $\delta = 0$ for simplicity. By Taylor expanding $K_V(\omega)$ around $\omega = 0$,[a] we obtain $K_V(\omega) = K_{V0} + K_{V1}\omega + \cdots$, with expansion coefficients $K_{Vj} = (\partial^j K_V(\omega)/\partial\omega^j)|_{\omega=0}$ $(j = 0, 1, \ldots)$. Here $K_{V0} = \mathrm{Re}\, K_{V0} + i\,\mathrm{Im}K_{V0}$ gives the phase shift per unit length and absorption coefficient and ReK_{V1} determines the group velocity V_g $(\equiv 1/\mathrm{Re}K_{V1})$.

Shown in Figs. 2(a) and 2(b) are respectively the real part and imaginary part of $K_V(\omega)$, which characterize the dispersion and absorption of the system, respectively. The dashed lines are results in the absence of the SGC ($\eta = 0$) while the solid lines are results with the maximum SGC ($\eta = 1$). System parameters are chosen as $\kappa = 1.0 \times 10^9$ cm^{-1} s^{-1}, $\Gamma = 1.0 \times 10^7$ s^{-1} and $\Delta = 1.0 \times 10^7$ s^{-1}. From Fig. 2 we see that: (i) In the region around $\omega = 0$ the probe field displays a drastic change of dispersion (and hence a drastic reduction of group velocity) [panel (a)] and complete elimination of absorption [panel (b)]. (ii) Steepness of the group velocity and reduction of the absorption are much more significant with the maximum SGC than those without the SGC.

Now we discuss the SGC effect in the probe-field absorption in more detail. From Fig. 2(b) we find that the reduction in absorption occurs around $\omega = 0$ even when SGC is absent, resulting in a doublet structure of the absorption spectrum. This is because the reduction may be a consequence of two similar, but very different mechanisms, i.e., SGC and ATS, appearing in the same system. The depth and width of transparency windows produced by above two mechanisms are, however, quite different.

For analyzing the above mentioned two mechanisms, we employ the spectrum decomposition method developed in Refs. 28–30 to transform $K(\omega)$ into the form of a superposition of two resonant responses associated with the transitions from the ground state to corresponding decaying-dressed states:

$$K_V(\omega) = \frac{\omega}{c} + R_+ + R_- \,, \tag{11}$$

[a]The frequency and wavenumber of the probe field are given by $\omega_p + \omega$ and $k_p + K(\omega)$, respectively. Thus $\omega = 0$ corresponds to the probe field.

where,

$$R_{\pm} = -\kappa \frac{A_{\pm}}{\omega - \omega_{\pm}}\,, \tag{12}$$

represent two resonances, with poles:

$$\omega_{\pm} = -i\frac{\Gamma}{2} \pm \sqrt{\Delta^2 - \eta^2\Gamma^2/4}\,, \tag{13}$$

and amplitudes

$$A_{\pm} = \pm \frac{\omega_{\pm} + i(1-\eta)\Gamma/2}{\sqrt{\Delta^2 - \eta^2\Gamma^2/4}}\,. \tag{14}$$

The total absorption $\mathrm{Im}\, K_V(\omega)$ can be discussed in the following regions determined on parameters Γ, Δ and η:

(i) SGC region: If $2\Delta/\Gamma < \eta \leq 1$, $\omega_{\pm}$ are purely imaginary given as:

$$\omega_{\pm} = i\left[-\frac{\Gamma}{2} \pm \sqrt{\eta^2\Gamma^2/4 - \Delta^2}\right] \equiv iW_{\pm}\,, \tag{15}$$

and $A_{\pm}$ are purely real given as:

$$A_{\pm} = \pm \frac{W_{\pm} + (1-\eta)\Gamma/2}{\sqrt{\eta^2\Gamma^2/4 - \Delta^2}}\,. \tag{16}$$

Thus the total absorption can be expressed as:

$$\mathrm{Im}\, K_V(\omega) = -\kappa\left(\frac{A_+W_+}{\omega^2 + W_+^2} + \frac{A_-W_-}{\omega^2 + W_-^2}\right). \tag{17}$$

From Eq. (17) we note that the absorption spectrum possesses following characteristics. First, the total absorption spectrum is made of two Lorentzians, which completely overlap (i.e., peak on peak). Second, one Lorentzian is positive indicating the absorption whereas the other one is negative indicating the gain. Third, the positive Lorentzian is wider than the negative one (i.e., $|W_-| > |W_+|$). Thus, the dip in the total absorption can be regarded as an "imprint" of one Lorentzian into the other, which is a result of a destructive interference between the two Lorentzians. This destructive interference is a signature of SGC.

(ii) SGC-ATS crossover region: If $0 < \eta < 2\Delta/\Gamma$, both $\omega_{\pm}$ and $A_{\pm}$ are complex written as $\omega_{\pm} = \pm\omega_0 - i\Gamma/2$ and $A_{\pm} = 1 \mp iB$, with $\omega_0 = \sqrt{\Delta^2 - \eta^2\Gamma^2/4}$ and $B = \eta\Gamma/(2\omega_0)$. The total absorption can be expressed as:

$$\begin{aligned}\mathrm{Im}\, K_V(\omega) = \kappa\Bigg[&\frac{\Gamma/2}{(\omega-\omega_0)^2 + \Gamma^2/4} + \frac{\Gamma/2}{(\omega+\omega_0)^2 + \Gamma^2/4} \\ &+ \frac{(\omega-\omega_0)B}{(\omega-\omega_0)^2 + \Gamma^2/4} - \frac{(\omega+\omega_0)B}{(\omega+\omega_0)^2 + \Gamma^2/4}\Bigg].\end{aligned} \tag{18}$$

We see that in this region the absorption spectrum is made of four terms. The first two terms are Lorentzians with the same width (determined by $\Gamma/2$) corresponding to two absorption resonances from the ground state to the pair of excited states.

A dip in the total absorption can be interpreted as a gap between two resonances, which is a typical character of ATS.[29] The next two terms are interference terms. Because they lower the dip formed by the first two terms, a destructive interference (i.e., SGC) occurs. A joint contribution from SGC and ATS occurs in the SGC-ATS crossover region.

(iii) ATS region: If $\eta \simeq 0$, one has $\omega_0 \simeq \Delta$, thus the next two terms (SGC terms) in Eq. (18) can be neglected and no SGC occurs. The total absorption spectrum consists of two Lorentzians

$$\mathrm{Im}\, K_V(\omega) = \kappa \frac{\Gamma}{2} \left[\frac{1}{(\omega - \Delta)^2 + \Gamma^2/4} + \frac{1}{(\omega + \Delta)^2 + \Gamma^2/4} \right], \tag{19}$$

a typical character of ATS. Thus in this situation a dip in the total absorption contributes by ATS effect.

The absorption properties in different regions are summarized in Fig. 3. In panel (a), we show the imaginary part of two resonances, $\mathrm{Im}(R_1) = -\kappa A_+ W_+/(\omega^2 + W_+^2)$ (dash line) and $\mathrm{Im}(R_2) = -\kappa A_- W_-/(\omega^2 + W_-^2)$ (dashed-dotted line) and their combination as the total absorption in the SGC region (solid line) by taking $\eta = 1$. In panel (b), we show the first two terms (ATS terms; dashed-dotted lines), the next two terms (SGC terms; dashed line), and their combination as the total absorption in the SGC-ATS crossover region (solid line) by taking $\eta = 0.6$. In panel (c) we show the total absorption in the ATS region by taking $\eta = 0$. System parameters are chosen as $\kappa = 1.0 \times 10^9$ cm^{-1} s^{-1}, $\Gamma = 1.0 \times 10^7$ s^{-1}, $\delta = 0$ and $\Delta = 4.5 \times 10^6$ s^{-1}. We see that the crossover from SGC to ATS can be achieved by changing the magnitude of SGC (i.e., η).

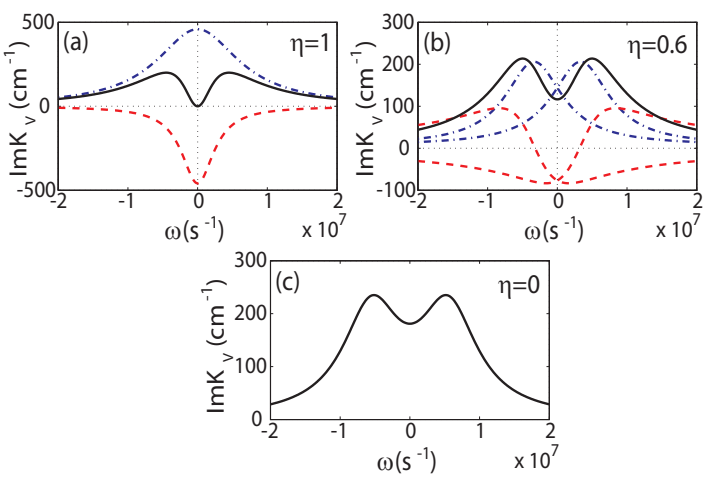

Fig. 3. (a) $\mathrm{Im}(R_1)$ (dash line), $\mathrm{Im}(R_2)$ (dashed-dotted line), and the total absorption $\mathrm{Im}\, K_V$ (solid line) as functions of ω with $\eta = 1$. (b) The first two terms in Eq. (18) (ATS terms; dashed-dotted lines), the next two terms in Eq. (18) (SGC terms; dashed lines), and $\mathrm{Im}\, K_V$ (solid line) as functions of ω with $\eta = 0.6$. (c): $\mathrm{Im}\, K_V$ as a function of ω with $\eta = 0$. Panels (a)–(c) correspond to SGC, SGC-ATS crossover and ATS regions, respectively.

2.3. *Warm atoms*

Now we consider the V-type system with warm atoms. The linear dispersion relation taken into account the Doppler effect reads:

$$\mathcal{K}_V(\omega) = \frac{\omega}{c} - \kappa \int_{-\infty}^{\infty} dv f(v) \frac{2\omega - 2k_p v + i(1-\eta)\Gamma}{\mathcal{D}_V(\omega)}\,, \tag{20}$$

where $\mathcal{D}_V(\omega) = (\omega - k_p v + \Delta + i\Gamma/2)(\omega - k_p v - \Delta + i\Gamma/2) + \eta^2\Gamma^2/4$.

The integration in Eq. (20) with the Gaussian velocity distribution leads to some complicated combination of error functions, which is inconvenient for a simple and clear analytical approach. As did by Lee *et al.*,[31] in the following we use the modified Lorentzian velocity distribution:

$$f(v) = \frac{v_T}{\sqrt{\pi}(v^2 + v_T^2)}\,. \tag{21}$$

Then Eq. (20) can be solved analytically by using a contour integral in complex plane.

Notice that Eq. (20) has four first-order poles

$$k_p v = \pm i k_p v_T\,, \quad k_p v = \omega \mp \sqrt{\Delta^2 - \eta^2\Gamma^2/4} + i\frac{\Gamma}{2} \tag{22}$$

and only one of them is located in the lower half complex plane, i.e., $k_p v = -ik_p v_T \equiv -i\Delta\omega_D$, where $\Delta\omega_D$ represents the Doppler width. The integration in (20) can be calculated by the contour that goes along the real axis from r to $-r$ and then counterclockwise along a semicircle centered at 0 from $-r$ to r in the lower half complex plane under the limit $r \to \infty$ (see Fig. 4). According to residue theorem,[32] we obtain the result:

$$\mathcal{K}_V(\omega) = \frac{\omega}{c} - \sqrt{\pi}\kappa \frac{2\omega + i[2\Delta\omega_D + (1-\eta)\Gamma]}{\tilde{\mathcal{D}}_V(\omega)}\,, \tag{23}$$

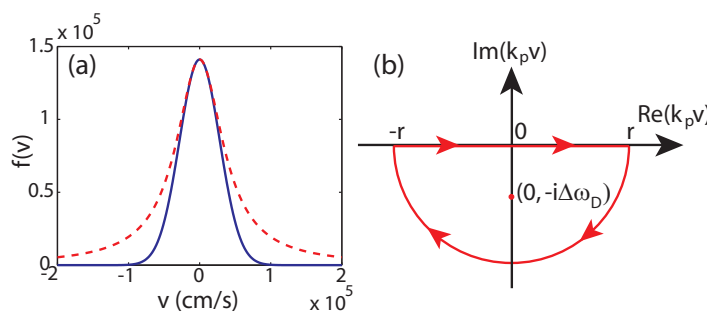

Fig. 4. (a) Gaussian velocity distribution (Eq. (8); solid line) and the modified Lorentzian velocity distribution (Eq. (21); dashed line) for $v_T = 4 \times 10^4$ cm/s. The central part of the modified Lorentzian velocity distribution coincides with that of the Gaussian velocity distribution. (b) The pole $(0, -i\Delta\omega_D)$ in the lower complex half plane of the integrand in Eq. (20). The closed curve with arrows is the contour chosen for calculating the integration in Eq. (20) by using residue theorem.

where $\tilde{\mathcal{D}}_V = [\omega + \Delta + i(2\Delta\omega_D + \Gamma)/2][\omega - \Delta + i(2\Delta\omega_D + \Gamma)/2] + \eta^2\Gamma^2/4$.

By spectrum decomposition similar to that used in the last subsection, we obtain:

$$\mathcal{K}_V(\omega) = \frac{\omega}{c} + \mathcal{R}_+ + \mathcal{R}_- \,, \tag{24}$$

where

$$\mathcal{R}_\pm = -\sqrt{\pi}\kappa \frac{\mathcal{A}_\pm}{\omega - \tilde{\omega}_\pm} \tag{25}$$

with

$$\tilde{\omega}_\pm = -i\frac{2\Delta\omega_D + \Gamma}{2} \pm \sqrt{\Delta^2 - \eta^2\Gamma^2/4}\,, \tag{26}$$

$$\mathcal{A}_\pm = \pm \frac{\tilde{\omega}_\pm + i[2\Delta\omega_D + (1-\eta)\Gamma]/2}{\sqrt{\Delta^2 - \eta^2\Gamma^2/4}}\,. \tag{27}$$

The total absorption $\mathrm{Im}\,\mathcal{K}_V(\omega)$ can be discussed in the following parameter regions:

(i) SGC region: If $2\Delta/\Gamma < \eta \leq 1$, the total absorption can be expressed as:

$$\mathrm{Im}\,\mathcal{K}_V(\omega) = -\sqrt{\pi}\kappa \left(\frac{\mathcal{A}_+\mathcal{W}_+}{\omega^2 + \mathcal{W}_+^2} + \frac{\mathcal{A}_-\mathcal{W}_-}{\omega^2 + \mathcal{W}_-^2} \right) , \tag{28}$$

where

$$\mathcal{W}_\pm = -\frac{2\Delta\omega_D + \Gamma}{2} \pm \sqrt{\eta^2\Gamma^2/4 - \Delta^2}\,, \tag{29}$$

$$\mathcal{A}_\pm = \pm \frac{\mathcal{W}_\pm + [2\Delta\omega_D + (1-\eta)\Gamma]/2}{\sqrt{\eta^2\Gamma^2/4 - \Delta^2}}\,. \tag{30}$$

The dip in the total absorption is a result of a destructive interference between two Lorentzians, which is a signature of SGC.

(ii) SGC-ATS crossover region: If $0 < \eta < 2\Delta/\Gamma$, the total absorption can be expressed as:

$$\begin{aligned} \mathrm{Im}\,\mathcal{K}_V(\omega) = \sqrt{\pi}\kappa \Bigg[& \frac{\mathcal{W}}{(\omega - \omega_0)^2 + \mathcal{W}^2} + \frac{\mathcal{W}}{(\omega + \omega_0)^2 + \mathcal{W}^2} \\ & + \frac{(\omega - \omega_0)B}{(\omega - \omega_0)^2 + \mathcal{W}^2} - \frac{(\omega + \omega_0)B}{(\omega + \omega_0)^2 + \mathcal{W}^2} \Bigg], \end{aligned} \tag{31}$$

where ω_0 and B are the same with those defined in (18) and $\mathcal{W} = (2\Delta\omega_D + \Gamma)/2$. The dip in the total absorption is a result of a joint contribution from the ATS (the first two terms) and the SGC (the next two terms).

(iii) ATS region: If $\eta \simeq 0$, the total absorption can be expressed as two Lorentzians

$$\mathrm{Im}\,\mathcal{K}_V(\omega) = \sqrt{\pi}\kappa \left[\frac{\mathcal{W}}{(\omega - \Delta)^2 + \mathcal{W}^2} + \frac{\mathcal{W}}{(\omega + \Delta)^2 + \mathcal{W}^2} \right] . \tag{32}$$

Thus the dip in the total absorption is produced only by ATS effect.

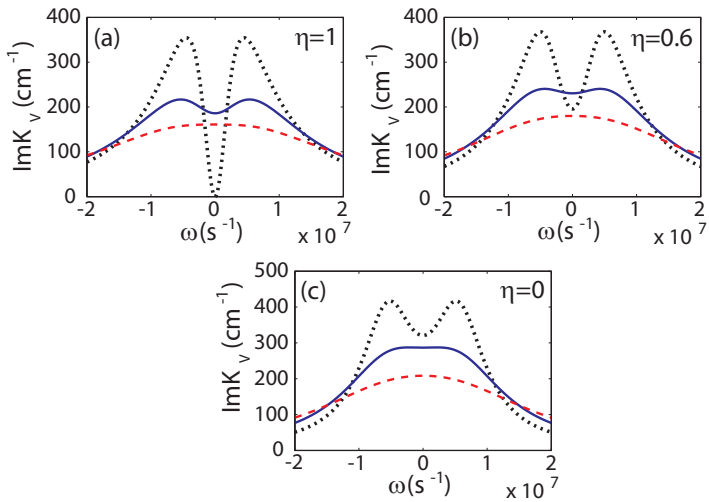

Fig. 5. The total absorption $\mathrm{Im}\mathcal{K}_V$ with (a) $\eta = 1$ (SGC region), (b) $\eta = 0.6$ (SGC-ATS crossover region) and (c) $\eta = 0$ (ATS point) for warm atoms. In each panel, the curves are obtained with $\Delta\omega_D = 0\ \mathrm{s}^{-1}$ (dotted line), $0.5 \times 10^7\ \mathrm{s}^{-1}$ (solid line) and $1.0 \times 10^7\ \mathrm{s}^{-1}$ (dashed line).

The absorption properties in different regions are summarized in Fig. 5. The total absorptions with $\Delta\omega_D = 0\ \mathrm{s}^{-1}$, $0.5 \times 10^7\ \mathrm{s}^{-1}$ and $1.0 \times 10^7\ \mathrm{s}^{-1}$ are displayed in each panels. Other parameters are the same as those used in Fig. 3. From Fig. 5, we obtain the following conclusions. First, the Doppler effect does not change the property of SGC-ATS crossover. Second, when $\Delta\omega_D \to 0$, Eqs. (28), (31) and (32) are respectively reduced to Eqs. (17)–(19). Third, the transparency window in the absorption spectrum becomes smaller due to the Doppler effect.

3. Λ- and Ξ-Type Systems

3.1. Λ-*type system*

We now consider a three-level Λ-type system. In such a system, a weak probe field with the form $\mathbf{E}_p(\mathbf{r}, t) = \mathbf{e}_p\mathcal{E}_p(\mathbf{r}, t)e^{i(k_p z-\omega_p t)} + \mathrm{c.c}$ couples the excited state $|3\rangle$ to the two ground states $|1\rangle$ and $|2\rangle$, with corresponding spontaneous decay rates Γ_1 and Γ_2, respectively [see Fig. 6(a)]. A SGC occurs by the quantum interference between two spontaneous decay channels from $|3\rangle$ to $|1\rangle$ and from $|3\rangle$ to $|2\rangle$.[33]

The atomic dynamics is described by the density matrix equations:

$$\dot{\rho}_{11} = \Gamma_1\rho_{33} + ip\Omega_p^*\rho_{31} - ip\Omega_p\rho_{13}\,, \tag{33}$$

$$\dot{\rho}_{22} = \Gamma_2\rho_{33} + i\Omega_p^*\rho_{32} - i\Omega_p\rho_{23}\,, \tag{34}$$

$$\dot{\rho}_{33} = -(\Gamma_1 + \Gamma_2)\rho_{33} - ip\Omega_p^*\rho_{31} + ip\Omega_p\rho_{13} - i\Omega_p^*\rho_{32} + i\Omega_p\rho_{23}\,, \tag{35}$$

$$\dot{\rho}_{21} = -i2\Delta\rho_{21} + i\Omega_p^*\rho_{31} - ip\Omega_p\rho_{23} + \eta\sqrt{\Gamma_1\Gamma_2}\rho_{33}\,, \tag{36}$$

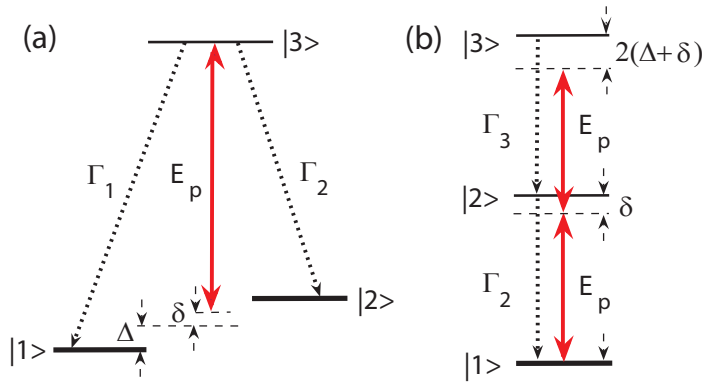

Fig. 6. (a) Three-level Λ-type and (b) Ξ-type systems. $|j\rangle$ $(j = 1, 2, 3)$ are atomic bare states, $\mathbf{E}_p$ is weak probe laser field, Δ and δ are detunings and Γ_j are decay rates of relevant states.

$$\dot{\rho}_{31} = \left[-i(\Delta+\delta) - \frac{\Gamma_1+\Gamma_2}{2}\right]\rho_{31} + ip\Omega_p(\rho_{11}-\rho_{33}) + i\Omega_p\rho_{21}\,, \tag{37}$$

$$\dot{\rho}_{32} = \left[i(\Delta-\delta) - \frac{\Gamma_1+\Gamma_2}{2}\right]\rho_{32} + i\Omega_p(\rho_{22}-\rho_{33}) + ip\Omega_p\rho_{12}\,, \tag{38}$$

where $\Omega_p = \mathbf{e}_p \cdot \mathbf{d}_{13}\mathcal{E}_p/\hbar$ is half Rabi frequency of the probe field, $\Delta = (E_2 - E_1)/(2\hbar)$ is half frequency difference of two closely spaced ground-state levels and $\delta = -\mathbf{k}_p \cdot \mathbf{v} + (2E_3 - E_1 - E_2)/(2\hbar) - \omega_p$ is one-photon detuning [see Fig. 6(a)]. The SGC effect is described by the factor $\eta\sqrt{\Gamma_1\Gamma_2}/2$, with $\eta = \mathbf{d}_{13}\cdot\mathbf{d}_{23}/|\mathbf{d}_{13}||\mathbf{d}_{23}|$. The factor $p = |\mathbf{e}_p \cdot \mathbf{d}_{13}|/|\mathbf{e}_p \cdot \mathbf{d}_{23}| = \cos\theta_1/\cos\theta_2$ $(|\mathbf{d}_{13}| \simeq |\mathbf{d}_{23}|)$.

The equation of motion for Ω_p is:

$$i\left(\frac{\partial}{\partial z} + \frac{1}{c}\frac{\partial}{\partial t}\right)\Omega_p + \int_{-\infty}^{\infty} dv f(v)(\kappa_{13}p\rho_{31} + \kappa_{23}\rho_{32}) = 0\,. \tag{39}$$

For simplicity, we assume in the following that $\Gamma_1 \approx \Gamma_2 = \Gamma$, $\kappa_{13} \simeq \kappa_{23} = \kappa$ and $p = 1$.

When the probe field is absent, the steady-state solution of the system reads $\rho_{11}^{(0)} + \rho_{22}^{(0)} = 1$ and $\rho_{33}^{(0)} = \rho_{mn}^{(0)} = 0$ $(m, n = 1, 2, 3; m \neq n)$.

Using MB Eqs. (33)–(39), in the case of cold atoms ($v \to 0$ and $f(v) \to \delta(v)$), the linear dispersion relation of the system reads:

$$K_\Lambda(\omega) = \frac{\omega}{c} - \kappa\left[\frac{\rho_{11}^{(0)}}{\omega - \Delta + i\Gamma} + \frac{\rho_{22}^{(0)}}{\omega + \Delta + i\Gamma}\right] \tag{40}$$

and the total absorption

$$\mathrm{Im}\, K_\Lambda(\omega) = \kappa\Gamma\left[\frac{\rho_{11}^{(0)}}{(\omega-\Delta)^2 + \Gamma^2} + \frac{\rho_{22}^{(0)}}{(\omega+\Delta)^2 + \Gamma^2}\right]. \tag{41}$$

In the case of warm atoms ($v > 0$ and $f(v) = (v_T/\sqrt{\pi}(v^2 + v_T^2))$), the linear dispersion relation of the system reads:

$$\mathcal{K}_\Lambda(\omega) = \frac{\omega}{c} - \kappa \int_{-\infty}^{\infty} dv f(v) \left[\frac{\rho_{11}^{(0)}}{\omega - k_p v - \Delta + i\Gamma} + \frac{\rho_{22}^{(0)}}{\omega - k_p v + \Delta + i\Gamma} \right], \quad (42)$$

where the integrand has only one pole in the lower half complex plane, i.e., $k_p v = -i\Delta\omega_D$. Thus, Eq. (42) can be easily solved as:

$$\mathcal{K}_\Lambda(\omega) = \frac{\omega}{c} - \sqrt{\pi}\kappa \left[\frac{\rho_{11}^{(0)}}{\omega - \Delta + i(\Delta\omega_D + \Gamma)} + \frac{\rho_{22}^{(0)}}{\omega + \Delta + i(\Delta\omega_D + \Gamma)} \right], \quad (43)$$

and the total absorption

$$\mathrm{Im}\,\mathcal{K}_\Lambda(\omega) = \sqrt{\pi}\kappa(\Delta\omega_D + \Gamma) \left[\frac{\rho_{11}^{(0)}}{(\omega - \Delta)^2 + (\Delta\omega_D + \Gamma)^2} + \frac{\rho_{22}^{(0)}}{(\omega + \Delta)^2 + (\Delta\omega_D + \Gamma)^2} \right]. \quad (44)$$

Both Eqs. (41) and (44) consist of two Lorentzians corresponding to resonances between $|3\rangle$ and $|1\rangle$ and between $|3\rangle$ and $|2\rangle$, respectively. Thus, a dip in the absorption spectrum of the probe field is produced only by the ATS. This tells us the SGC has no effect on the linear dispersion and absorption properties of the Λ-type system.

3.2. Ξ-*type system*

For completeness, we finally consider a three-level Ξ-type system, as shown in Fig. 6(b), in which a weak probe field with the form $\mathbf{E}_p(\mathbf{r}, t) = \mathbf{e}_p \mathcal{E}_p(\mathbf{r}, t) e^{i(k_p z - \omega_p t)} +$ c.c couples the ground state $|1\rangle$ to the intermediate state $|2\rangle$ and simultaneously couples the state $|2\rangle$ to the excited state $|3\rangle$, as suggested in Ref. 34. States $|2\rangle$ and $|3\rangle$ decay to $|1\rangle$ and $|2\rangle$ with decay rates Γ_1 and Γ_2, respectively. The density matrix equations governing the atomic dynamics are given by

$$\dot{\rho}_{11} = \Gamma_2 \rho_{22} + i\Omega_p^* \rho_{21} - i\Omega_p \rho_{12}\,, \quad (45)$$

$$\dot{\rho}_{22} = -\Gamma_2 \rho_{22} + \Gamma_3 \rho_{33} - i\Omega_p^* \rho_{21} + i\Omega_p \rho_{12} - ip\Omega_p \rho_{23} + ip\Omega_p^* \rho_{32}\,, \quad (46)$$

$$\dot{\rho}_{33} = -\Gamma_3 \rho_{33} + ip\Omega_p \rho_{23} - ip\Omega_p^* \rho_{32}\,, \quad (47)$$

$$\dot{\rho}_{21} = \left(-i\delta - \frac{\Gamma_2}{2} \right) \rho_{21} + i\Omega_p(\rho_{11} - \rho_{22}) + ip\Omega_p^* \rho_{31} + \eta \frac{\sqrt{\Gamma_2 \Gamma_3}}{2} \rho_{32}\,, \quad (48)$$

$$\dot{\rho}_{31} = \left[-i2\,(\Delta + \delta) - \frac{\Gamma_3}{2} \right] \rho_{31} + ip\Omega_p \rho_{21} - i\Omega_p \rho_{32}\,, \quad (49)$$

$$\dot{\rho}_{32} = \left[-i(2\Delta + \delta) - \frac{\Gamma_2 + \Gamma_3}{2} \right] \rho_{32} + ip\Omega_p(\rho_{22} - \rho_{33}) - i\Omega_p^* \rho_{31}\,, \quad (50)$$

where $\Omega_p = |\mathbf{e}_p \cdot \mathbf{d}_{12}|\mathcal{E}_p/\hbar$ is half Rabi frequency of the probe field, $\Delta = (E_3 - 2E_2 + E_1)/(2\hbar)$ is half frequency difference of the transitions $|1\rangle \leftrightarrow |2\rangle$ and $|2\rangle \leftrightarrow |3\rangle$ and $\delta = (E_2 - E_1)/\hbar - \omega_p$ is one-photon detuning [see Fig. 6(b)]. The last term on the right-hand side of Eq. (48) comes from the SGC effect, with $\eta = \mathbf{d}_{12} \cdot \mathbf{d}_{23}/|\mathbf{d}_{12}||\mathbf{d}_{23}| = \cos\theta$. The factor $p = |\mathbf{e}_p \cdot \mathbf{d}_{23}|/|\mathbf{e}_p \cdot \mathbf{d}_{12}| = \cos\theta_1/\cos\theta_2$ ($|\mathbf{d}_{23}| \simeq |\mathbf{d}_{12}|$).

The equation of motion for Ω_p is:

$$i\left(\frac{\partial}{\partial z} + \frac{1}{c}\frac{\partial}{\partial t}\right)\Omega_p + \int_{-\infty}^{\infty} dv f(v)(\kappa_{12}\rho_{21} + \kappa_{23}p\rho_{32}) = 0\,. \tag{51}$$

For simplicity, we assume in the following that $\Gamma_2 \approx \Gamma_3 = \Gamma$, $\kappa_{12} \simeq \kappa_{23} = \kappa$ and $p = 1$.

When the probe field is absent, the steady-state solution of the system reads:

$$\rho_{11}^{(0)} = 1 \quad \text{and} \quad \rho_{22}^{(0)} = \rho_{33}^{(0)} = \rho_{mn}^{(0)} = 0 \quad (m, n = 1, 2, 3; m \neq n)\,.$$

Using MB Eqs. (45)–(51) we obtain the linear dispersion relation of the system

$$K_\Xi(\omega) = \frac{\omega}{c} - \kappa\frac{1}{\omega + i\Gamma/2}\,, \tag{52}$$

for cold atoms and

$$\mathcal{K}_\Xi(\omega) = \frac{\omega}{c} - \kappa\frac{1}{\omega + i(\Delta\omega_D + \Gamma/2)}\,, \tag{53}$$

for warm atoms. Thus, the total absorptions in the cases of cold atoms and warm atoms are:

$$\mathrm{Im}\, K_\Xi(\omega) = \kappa\frac{\Gamma/2}{\omega^2 + \Gamma^2/4} \tag{54}$$

and

$$\mathrm{Im}\, \mathcal{K}_\Xi(\omega) = \kappa\frac{\Delta\omega_D + \Gamma/2}{\omega^2 + (\Delta\omega_D + \Gamma/2)^2}\,, \tag{55}$$

respectively. From these results, we see that the Ξ-type system possess neither SGC nor ATS because there is no dip in the probe-field absorption spectrum.

4. Summary

The SGC occurs in systems having near-degenerated levels with the same angular momentum quantum numbers J and m_J and nonorthogonal dipole moments, which are usually rare in atomic media.[35] However, in a recent experiment,[36] a SGC has been observed in a rubidium atoms with N- and inverted Y-type level configurations. In addition, the quantum interference via SGC can be observed in many other systems such as semiconductor quantum wells and quantum dots,[37–39] autoionizing media,[40] and anisotropic vacuum.[41] Our theoretical approach presented above can be easily generalized to these systems with the SGC. The next step is to extend our theoretical approach to four-level systems.

In summary, in this article we have investigated SGC and ATS in various three-level atomic systems. By detailed analytical calculations on absorption spectrum of probe laser field, we have shown that in V-type system the SGC can completely eliminate the absorption of the probe field and at the same time significantly reduce the group velocity. Using residue theorem and spectrum decomposition method, we have found that there exists a SGC-ATS crossover for both cold and warm atoms when the magnitude of SGC is changed. Different contributions from SGC and ATS to probe-field absorption spectrum were clearly clarified in different parameter regions. In addition, our research shows that there is no SGC and hence no SGC-ATS crossover in Λ- and Ξ-type systems. The results obtained in this work may guide new experimental findings related to SGC and have promising applications in optical information processing.

Acknowledgments

This work was supported by the NSF-China under Grant numbers 11174080 and 11105052, and by the Open Fund from the State Key Laboratory of Precision Spectroscopy, ECNU.

References

1. M. Fleischhauer, A. Imamoglu and J. P. Marangos, *Rev. Mod. Phys.* **77**, 633 (2005), and references therein.
2. A. I. Lvovsky, B. C. Sanders and W. Tittel, *Nat. Photon.* **3**, 706 (2009).
3. C. Ottaviani *et al.*, *Phys. Rev. Lett.* **90**, 197902 (2003).
4. C. Hang *et al.*, *Phys. Rev. A* **74**, 012319 (2006).
5. Y. Wu and L. Deng, *Phys. Rev. Lett.* **93**, 143904 (2004).
6. G. Huang, L. Deng and M. G. Payne, *Phys. Rev. E.* **72**, 016617 (2005).
7. G. S. Agarwal, *Quantum Optics, Springer Tracts in Modern Physics*, Vol. 70 (Springer, 1974).
8. S. E. Harris, *Phys. Rev. Lett.* **62**, 1033 (1989).
9. A. Imamoğlu, *Phys. Rev. A* **40**, 2835 (1989).
10. J. H. Wu and J. Y. Gao, *Phys. Rev. A* **65**, 063807 (2002).
11. Y. Bai *et al.*, *Phys. Rev. A* **69**, 043814 (2004).
12. S. Menon and G. S. Agarwal, *Phys. Rev. A* **57**, 4014 (1998).
13. S. Y. Zhu, R. C. F. Chan and C. P. Lee, *Phys. Rev. A* **52**, 710 (1995).
14. S. Y. Zhu and M. O. Scully, *Phys. Rev. Lett.* **76**, 388 (1996).
15. P. Zhou and S. Swain, *Phys. Rev. Lett.* **77**, 3995 (1996).
16. E. Paspalakis and P. L. Knight, *Phys. Rev. Lett.* **81**, 293 (1998).
17. K. T. Kapale *et al.*, *Phys. Rev. A* **67**, 023804 (2003).
18. E. Paspalakis, N. J. Kylstra and P. L. Knight, *Phys. Rev. Lett.* **82**, 2079 (1999).
19. I. Gonzalo *et al.*, *Phys. Rev. A* **72**, 033809 (2005).
20. Y. P. Niu and S. Q. Gong, *Phys. Rev. A* **73**, 053811 (2006).
21. D. G. Norris *et al.*, *Phys. Rev. Lett.* **105**, 123602 (2010).
22. Z. Tang, G. Li and Z. Ficek, *Phys. Rev. A* **82**, 063837 (2010).
23. R. G. Wan *et al.*, *Phys. Rev. A* **83**, 033824 (2011).
24. C. Hang and G. Huang, *J. Opt. Soc. Am. B* **29**, 2009 (2012).
25. S. R. Autler and C. R. Townes, *Phys. Rev.* **100**, 703 (1955).

26. C. Cohen-Tannoudji and S. Reynaud, *J. Phys. B* **10**, 2311 (1977).
27. D. A. Cardimona, M. G. Raymer and C. R. Stroud Jr., *J. Phys. B* **15**, 65 (1982).
28. P. M. Anisimov, J. P. Dowling and B. C. Sanders, *Phys. Rev. Lett.* **107**, 163604 (2011).
29. T. Y. Abi-Salloum, *Phys. Rev. A* **81**, 053836 (2010).
30. C. Tan, C. Zhu and G. Huang, *J. Phys. B: At. Mol. Opt. Phys.* **46**, 025103 (2013).
31. H. Lee *et al.*, *Appl. Phys. B* **76**, 33 (2003).
32. F. W. Byron and R. W. Fuller, *Mathematics in Classical and Quantum Physics*, Vol. 2 (Addison-Wesley, 1969), Chap. 6.
33. J. Javanainen, *Europhys. Lett.* **17**, 407 (1992).
34. Z. Ficek, B. J. Dalton and P. L. Knight, *Phys. Rev. A* **51**, 4062 (1995).
35. H. R. Xia, C. Y. Ye and S. Y. Zhu, *Phys. Rev. Lett.* **77**, 1032 (1996).
36. S.-C. Tian *et al.*, *Opt. Commun.* **285**, 294 (2011).
37. J. Faist *et al.*, *Nat.* (*London*) **390**, 589 (1997).
38. H. Schmidt *et al.*, *Appl. Phys. Lett.* **70**, 3455 (1997).
39. J. H. Wu *et al.*, *Phys. Rev. Lett.* **95**, 057401 (2005).
40. T. Nakajima, *Phys. Rev. A* **63**, 043804 (2000).
41. G. S. Agarwal, *Phys. Rev. Lett.* **84**, 5500 (2000).